International Journal of Manufacturing and Materials Processing
Vol. 4: Issue 2
www.journalspub.com

Galerkin Method of Weighted Residual to Study on Enhanced Heat Transfer in Cylindrical Micro-Fins Heat Sink Using Artificial Surface Roughness

M.G. Sobamowo[1], K.F. Dukor[1], G.A. Oguntala[2]*
[1]Department of Mechanical Engineering, University of Lagos, Akoka, Lagos, Nigeria
[2]Faculty of Engineering and Informatics, School of Electrical Engineering and Computer Science, University of Bradford, West Yorkshire, United Kingdom

ABSTRACT
In this paper, a theoretical investigation is carried out on the use of artificial surface roughness for enhanced heat transfer and thermal management of cylindrical micro-fins with artificial surface roughness. The developed thermal models which are solved using Galerkin method of weighted residual, considered variable thermal properties according to linear, exponential and power laws. The approximate analytical solutions are used to carry out parametric studies and to establish the thermal performance enhancement of the rough fins over the existing smooth fins. Following the results of the simulations, it is established that the thermal efficiency of the micro-fin is significantly affected by the geometric ratio, nonlinear thermal conductivity parameter, thermo-geometric parameter and the surface roughness of the micro-fin. The results showed that geometric ratio and the surface roughness of the fin enhance the thermal performance of the micro-fin. The fin efficiency ratio as established in this present study is found to be greater than unity when the rough and the smooth fins are subjected to the same operations with the same geometrical, physical, thermal and material properties. Therefore, enhanced heat transfer and improved thermal management of electronic and thermal systems can be achieved through the use of artificial rough surface heat sink fins.

Keywords: artificial surface roughness, convective–radiative environment, enhanced heat transfer, heat sink, improved thermal management, micro-fin

Corresponding Author
E-mail: mikegbeminiyiprof@yahoo.com

INTRODUCTION
The quest and the production of high-performance electronic systems come with inherent thermal challenges. Considering the thermal challenges for the present and the next-generation electronics systems [1], the need for combating the heat generation has been increasing. Effective cooling technology or thermal management of microprocessors in most electronic devices including notebook and computers and in various thermal devices or componens in thermal equiptment has been one of the ultimate goals of the present advanced technology designers in electronics productions and design of thermal systems. To achieve the goals, both active and passive modes of cooling technologies have been deployed. However, the active modes of heat transfer enhancement or augmentation such as fans, blowers, fluid vibration, surface vibration, suction and jet impingement and electrostatic fields have proved not to be economically viable due to their operating costs. As alternative means of thermal cooling, the applications of passive methods such as extended surfaces and treated surfaces have shown to be very effective thermal management technology [2]. As one of the passive modes of the

thermal cooling technologies, fins or extended surfaces have used to enhance the rate of heat transfer from thermal and electronic systems. Ligrani et al. [3] presented a comparative study on different techniques for heat transfer augmentation. With the applications of extended surfaces, high thermal performance in both electronic and thermal systems have been recorded [4–16]. However, the quest for more highly efficient heat sinks or fins with reduced thermal resistance, i.e. lightweight, continues. In such search for an increased high performance, in their investigations, Zhou et al. [17] and Ventola et al. [2]advocated for the use of artificial surface roughness for transfer enhancement through extended surfaces. Moreover, the potential of enhanced thermal management and heat transfer augmentation of surfaces with artificial roughness have been evidently and experimentally reported. Consequently, different methods have been proposed and used to produce artificial surface roughness in heat transfer surfaces [18–22]. On paramteric studies, Bahrami [23] presented a study on the effects of random rough surface on thermal performance of micro-fin, while Diez et al. [24] applied power series to analyse the thermal performance of rough micro-fins of three different profiles, namely hyperbolic, trapezoidal and concave. However, apart from the fact that the analysis of the later authors only considered thermal performance conductive–convective fins, it was based on assumed constant thermal properties. Such an assumption is not valid when a large temperature difference exists between the fin base and its tip. To the best of our knowledge, a study on the enhanced thermal heat transfer and improved management of micro-fins with artificial surface roughness and variable thermal properties using Galerkin method of weighted residual has not been carried out. Therefore, this paper presents a study on the application of artificial rough surface fins for heat transfer enhnacement and improved thermal management of thermal systems using cylindrical rough pin micro-fins with variable thermal properties. Also, effects of roughness, variable thermal performance, convective heat transfer, radiative heat transfer on the thermal performance and heat transfer enhancement of themal systems are investigated theoretically.

FORMULATION

Consider a heat sink made up of a rough cylindrical micro-fin shown in Figure 1. Assume the fin is of dimension *L* and *t*, and exposed on both faces and subjected to a convective–radiative environment with temperature T_a, whilst no thermal contact resistance exists at the fin base.

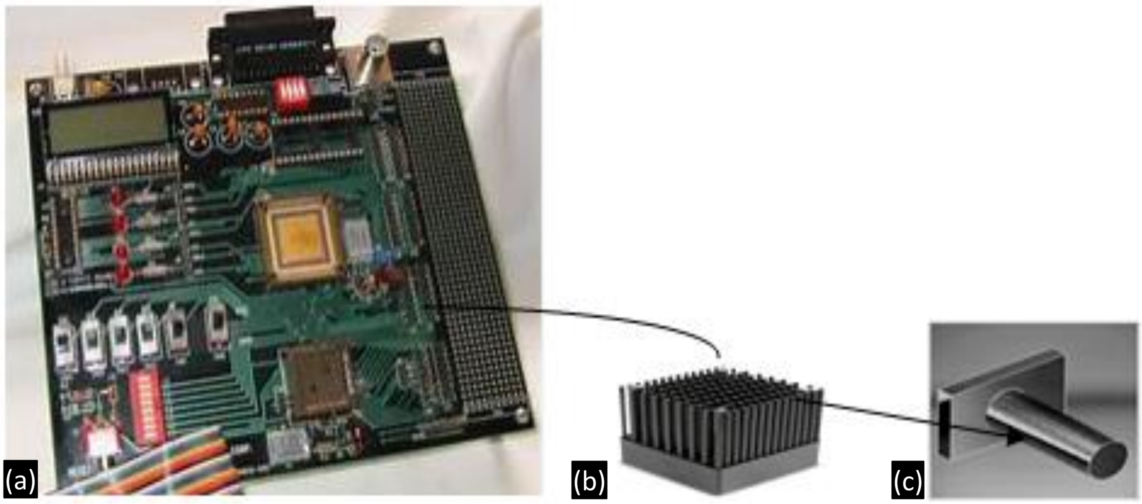

Fig. 1. *(a) A motherboard of an electronics made up of heat sinks. (b) Schematic diagram of heat sink fin. (c) Schematic of a rough surface heat sink.*

For the one-dimensional heat flow and following the assumptions stated above, the governing equations for the heat transfer in the fin is

$$\frac{d}{dx}\left(-k(T)A_c\frac{dT}{dx}\right)+h(T)P(T-T_\infty)=0. \tag{1}$$

The boundary conditions are given as

$$\begin{aligned} x=0,\quad & T=T_b. \\ x=L,\quad & \frac{dT}{dx}=0. \end{aligned} \tag{2}$$

The thermal conductivity of the micro-pin-fins can vary linearly as

$$k(T)=k_a(1+\lambda(\mathrm{T}-\mathrm{T}_\infty)), \tag{3a}$$

or exponentially as

$$k(T)=k_a e^{\lambda(T-T_\infty)}. \tag{3b}$$

The convective heat transfer coefficient will vary as

$$h(T)=h_b\left(\frac{T-T_\infty}{T_b-T_\infty}\right)^n. \tag{3c}$$

Substituting Equations (3a) and (3c), Equation (1) becomes

$$\begin{aligned} & k_a\frac{d\overline{A_c}}{dx}\frac{dT}{dx}+k_a\overline{A_c}\frac{d^2T}{dx^2}+k_a\lambda\left(T-T_\infty\right)\frac{d\overline{A_c}}{dx}\frac{dT}{dx}+k_a\lambda\overline{A_c}\left(\frac{dT}{dx}\right)^2+ \\ & k_a\lambda\overline{A_c}\left(T-T_\infty\right)\frac{d^2T}{dx^2}-\frac{h_bP\left(T-T_\infty\right)^{n+1}}{\left(T_b-T_\infty\right)^n}=0. \end{aligned} \tag{4}$$

If the thermal conductivity varies exponentially according to the law $k(T)=k_a e^{\lambda(T-T_\infty)}$, we have

$$k_a e^{\lambda(T-T_\infty)}\frac{d\overline{A_c}}{dx}\frac{dT}{dx}+k_a\lambda\overline{A_c}e^{\lambda(T-T_\infty)}\left(\frac{dT}{dx}\right)^2+k_a\overline{A_c}e^{\lambda(T-T_\infty)}\frac{d^2T}{dx^2}-\frac{h_bP\left(T-T_\infty\right)^{n+1}}{\left(T_b-T_\infty\right)^n}=0. \tag{5}$$

Table 1. *Heat transfer modes constants.*

Heat transfer mode	**Multi-boiling heat transfer constant, *n***
Laminar film boiling or condensation	-1/4
Laminar natural convection	1/4
Turbulent natural convection	1/3
Nucleate boiling	2
Radiation	3
Constant heat transfer coefficient	0

MATHEMATICAL MODELS FOR THE SURFACE ROUGHNESS

In order to develop mathematical models for the rough surface, it was assumed that the rough micro-fins have a random surface roughness that obeys the Gaussian probability distribution both in angular and longitudinal directions, as shown in Figures 2 and 3. Such an assumption is in line with the assumption in the work of Bahrami et al. [23] and Diez et al. [24]. Following the work of Diez et al. [24], it can easily be shown that

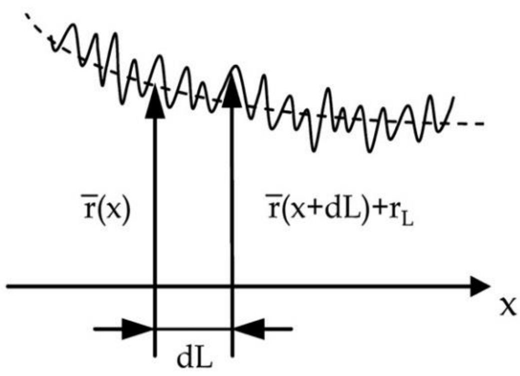

Fig. 2. *Details of a cross-section of generic pin fin of variable profile and rough surface.*

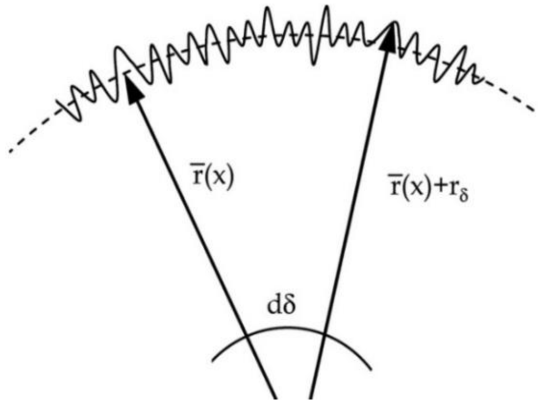

Fig. 3. *Details of longitudinal section of a generic pin fin of variable profile and rough surface.*

$$\frac{\bar{A}_c(x)}{A_c(x)} = 1 + 2\left(\frac{\sigma}{\bar{r}(x)}\right)^2, \quad (6)$$

$$\frac{d\bar{A}_c}{dx} \approx \frac{dA_c}{dx} + 2\pi\bar{r}\left(x\right)m_\sigma = 2\pi\bar{r}\left(x\right)\sqrt{1+m_\sigma^2}, \quad (7)$$

$$\bar{P}(x) = \frac{d\bar{A}_c}{dx} \approx 2\pi\bar{r}\left(x\right)\sqrt{1+m_\sigma^2}, \quad (8)$$

where, for a smooth perimeter, $P(x) = 2\pi\bar{r}\left(x\right)$,

$$P(x) = P\left(x\right)\sqrt{1+m_\sigma^2}, \quad (9)$$

and the mean absolute surface slope of the roughness component is given as

$$m_\sigma = \frac{1}{L}\int_0^L \left|\frac{\partial\left(r-r_b\right)}{dx}\right| dx. \quad (10)$$

Taking the relative roughness as $\mathcal{E}$, by using the radius at the fin base, we can define the roughness ratio as

$$\mathcal{E} = \frac{\sigma}{r_b}. \quad (11)$$

On substituting Equation (11) into Equation (6), we have

$$\bar{A}_c\left(x\right) = \left(1 + 2\left(\frac{r_b}{\bar{r}\left(x\right)}\right)^2 \mathcal{E}^2\right) A_c\left(x\right). \quad (12)$$

Substituting Equations (7)–(9) and (12) into Equation (5), we arrived at an energy equation for rough micro-fin as

$$\begin{aligned} &k_a \frac{dA_c}{dx}\frac{dT}{dx} + 2\pi\bar{r}m_\sigma \frac{dT}{dx} + A_c\frac{d^2T}{dx^2} + 2\varepsilon^2 A_c\left(\frac{r_b}{\bar{r}}\right)^2\frac{d^2T}{dx^2} + \lambda\left(T-T_\infty\right)\frac{dA_c}{dx}\frac{dT}{dx} \\ &+2\pi\bar{r}m_\sigma\lambda\left(T-T_\infty\right)\frac{dT}{dx} + \lambda A_c\left(\frac{dT}{dx}\right)^2 + 2\varepsilon^2 A_c\lambda\left(\frac{r_b}{\bar{r}}\right)^2\left(\frac{dT}{dx}\right)^2 + \\ &A_c\lambda\left(T-T_\infty\right)\frac{d^2T}{dx^2} + 2\varepsilon^2 A_c\lambda\left(\frac{r_b}{\bar{r}}\right)^2\left(T-T_\infty\right)\frac{d^2T}{dx^2} - \frac{h_b P\sqrt{1+m_\sigma{}^2}}{k_a}\frac{\left(T-T_\infty\right)^{n+1}}{\left(T_b-T_\infty\right)^n} = 0. \end{aligned} \quad (13)$$

For cylindrical coordinate, A_c is constant; therefore, $\frac{dA_c}{dx} = 0$,

where $\bar{r_c}(x) = r_b$, $P(x) = 2\pi r_b$ and $A_c(x) = \pi r_b{}^2$.

Substituting these into Equation (13),

$$\begin{aligned} &\frac{d^2T}{dx^2} + \frac{2m_\sigma}{r_b}\frac{dT_c}{dx} + \frac{2\lambda m_\sigma}{r_b}\left(T_c-T_\infty\right)\frac{dT_c}{dx} + \lambda\left(\frac{dT_c}{dx}\right)^2 + 2\varepsilon^2\frac{d^2T_c}{dx^2} + \\ &2\varepsilon^2\lambda\left(\frac{dT_c}{dx}\right)^2 + \lambda\left(T_c-T_\infty\right)\frac{d^2T_c}{dx^2} + 2\varepsilon^2\lambda\frac{d^2T_c}{dx^2} - \frac{h_b P\sqrt{1+m_\sigma{}^2}}{r_b k_a}\frac{\left(T-T_\infty\right)^{n+1}}{\left(T_b-T_\infty\right)^n} = 0. \end{aligned} \quad (14)$$

Also, for the rough micro-fins with exponentially varying thermal conductivity, we have

$$\left(\begin{aligned} &\lambda A_c e^{\lambda(T-T_\infty)}\left(\frac{dT}{dx}\right)^2 + 2\lambda\varepsilon^2 A_c e^{\lambda(T-T_\infty)}\left(\frac{r_b}{\bar{r}}\right)^2\left(\frac{dT}{dx}\right)^2 + e^{\lambda(T-T_\infty)}\frac{dA_c}{dx}\frac{dT}{dx} + \\ &2\pi\bar{r}m_\sigma e^{\lambda(T-T_\infty)}\frac{dT}{dx} + A_c e^{\lambda(T-T_\infty)}\frac{d^2T}{dx^2} + 2A_c\varepsilon^2\left(\frac{r_b}{\bar{r}}\right)^2 e^{\lambda(T-T_\infty)}\frac{d^2T}{dx^2} - \frac{h_b P\sqrt{1+m_\sigma{}^2}\left(T-T_\infty\right)^{n+1}}{k_a\left(T_b-T_\infty\right)^n} = 0 \end{aligned}\right). \quad (15)$$

For cylindrical coordinate, we arrived at

$$\lambda e^{\lambda(T_c-T_\infty)}\left(\frac{dT_c}{dx}\right)^2+2\lambda\varepsilon^2 e^{\lambda(T_c-T_\infty)}\left(\frac{dT_c}{dx}\right)^2+\frac{2m_\sigma}{r_b}e^{\lambda(T_c-T_\infty)}\frac{dT_c}{dx}+$$
$$e^{\lambda(T_c-T_\infty)}\frac{d^2T_c}{dx^2}+2\varepsilon^2 e^{\lambda(T_c-T_\infty)}\frac{d^2T_c}{dx^2}-\frac{2h_b\sqrt{1+m_\sigma{}^2}\left(T_c-T_\infty\right)^{n+1}}{k_a r_b\left(T_b-T_\infty\right)^n}=0. \tag{16}$$

Introducing the following dimensionless parameters into Equations (14) and (15),

$$\theta=\frac{T-T_a}{T-T_a},\quad X=\frac{x}{L},\quad \lambda\left(T-T_\infty\right)=\beta_\lambda,\quad M_c{}^2=\frac{h_bL^2}{k_ar_b},\quad \beta_c=\frac{x}{r_b}m_\sigma,\quad \alpha_c=\mathcal{E}^2; \tag{17}$$

we arrived at the dimensionless governing equations as for the rough micro-fin with linearly varying and exponentially varying thermal conductivity, respectively, as

$$\frac{d^2\theta_c}{dX^2}+\frac{2m_\sigma z_t}{r_b}\frac{d\theta_c}{dX}+\frac{2\beta_\lambda m_\sigma\theta_c z_t}{r_b}\frac{d\theta_c}{dX}+\beta_\lambda\left(\frac{d\theta_c}{dX}\right)^2+2\varepsilon^2\frac{d^2\theta_c}{dX^2}+$$
$$2\varepsilon^2\beta_\lambda\left(\frac{d\theta_c}{dX}\right)^2-\beta\theta_c\frac{d^2\theta_c}{dX^2}+2\varepsilon^2\lambda\frac{d^2\theta_c}{dX^2}-2M_c{}^2\sqrt{1+m_\sigma{}^2}\,\theta_c{}^{n+1} \tag{18}$$

and

$$\beta_\lambda e^{\beta_\lambda\theta_c}\left(\frac{d\theta_c}{dX}\right)^2+2\beta_\lambda\alpha_c e^{\beta_\lambda\theta_c}\left(\frac{d\theta_c}{dX}\right)^2+2\gamma_c e^{\beta_\lambda\theta_c}\frac{d\theta_c}{dX}+$$
$$e^{\beta_\lambda\theta_c}\frac{d^2\theta_c}{dX^2}+2\alpha_c e^{\beta_\lambda\theta_c}\frac{d^2\theta_c}{dX^2}-2X_c\theta_c{}^{n+1}=0. \tag{19}$$

If the fin is smooth and the thermal conductivity varies linearly, we have

$$\frac{d^2\theta_c}{d\psi^2}+\beta\theta\frac{d^2\theta_c}{d\psi^2}+\beta\left(\frac{d\theta_c}{d\psi}\right)^2-2M_c{}^2\theta^{n+1}=0. \tag{20}$$

For the smooth fin with exponentially varying thermal conductivity,

$$e^{\beta\theta_c}\frac{d^2\theta_c}{d\psi^2}+\beta e^{\beta\theta_c}\left(\frac{d\theta_c}{d\psi}\right)^2-2M_c{}^2\theta^{n+1}=0. \tag{21}$$

The dimensionless boundary conditions are given as

$$X=0,\quad \theta=1,$$
$$X=1,\quad \frac{d\theta}{dX}=0. \tag{22}$$

In this work, the geometric ratio is given as $\xi=\dfrac{r}{L}$.

METHOD OF SOLUTION: GALERKIN METHOD OF WEIGHTED RESIDUAL

The equations derived for the different profiles are nonlinear equations and it defiles the use of any closed form of solution. For this reason, an approximate analytical method or numerical method is ideal for solving such problem. In this study, the Galerkin method of weighted residual, which is a simple and powerful approximate method, has been chosen for use in this work. The developed thermal models are solved semi-analytically using Galerkin method of weighted residual. The procedures, applications and advantages of method can be found in Sobamowo [25] and Sobamowo et al. [26].

In this work, a quadratic trial solution of this method is adopted. The procedure of the method is described as follows:
The quadratic trial solution equation is given as

$$\theta = \alpha_1 + \alpha_2 X + \alpha_3 X^2, \tag{23}$$

where
$x \sim \psi$ or φ.
And considering the boundary condition,

$$\theta = 1 - \left[\left(\xi^2 - 2\xi \right) + 2\psi - \psi^2 \right] \alpha_3. \tag{24}$$

For the smooth surface with constant thermal properties,

$$\int_0^1 (\xi^2 - (2\xi) + (2\psi) - \psi^2) \cdot \left(\frac{d^2\theta_c}{d\psi^2} - 2M_c{}^2 \theta_c \right), \tag{25}$$

which gives

$$\int_0^1 (\xi^2 - (2\xi) + (2\psi) - \psi^2) \cdot \left(2\alpha_3 - 2M_c{}^2 \cdot \left(1 - (\xi^2 - (2\xi) + (2\psi) - \psi^2)\alpha_3 \right) \right). \tag{26}$$

From Equation (26), we arrived at

$$\alpha_3 = \frac{2M_c{}^2 \left(\xi^2 - 2\xi + \frac{2}{3} \right)}{2\xi^2 - 4\xi + 2M_h{}^2 \left(\xi^4 - 4\xi^3 + 6\xi^2 - 4\xi + \frac{17}{15} \right) + \frac{4}{3}}. \tag{27}$$

After substituting Equation (27) into Equation (24), we arrived at

$$\theta_c = 1 - \left((\xi^2 - (2\xi) + (2\psi) - \psi^2) \left(\frac{2M_c{}^2 \left(\xi^2 - 2\xi + \frac{2}{3} \right)}{2\xi^2 - 4\xi + 2M_h{}^2 \left(\xi^4 - 4\xi^3 + 6\xi^2 - 4\xi + \frac{17}{15} \right) + \frac{4}{3}} \right) \right). \tag{28}$$

Similarly, for the for the rough surface with constant thermal properties,

$$\theta_c = 1 - \left((\xi^2 - (2\xi) + (2\psi) - \psi^2) \left(\frac{2X_c \left(\frac{\xi^2}{3} - \frac{\xi}{3} + \frac{3}{10} \right)}{\begin{array}{c} 2\xi^2 - 4\xi - \beta_c \left(2\xi^2 - 4\xi + 1 \right) + \frac{4\alpha_c (3\xi^2 - 6\xi + 2)}{3} + \\ 2X_c \left(\xi^4 - 4\xi^3 + \frac{16\xi^2}{3} - \frac{8\xi}{3} + \frac{8}{15} \right) + \frac{4}{3} \end{array}} \right) \right). \tag{29}$$

For the smooth surface with linearly varying thermal properties,

$$\theta_c = 1 - \left((\xi^2 - (2\xi) + (2\psi) - \psi^2)(\alpha_3) \right), \tag{30}$$

where

$$\alpha_3 = \frac{\frac{\beta_\lambda}{4} + 2\xi + \frac{12M^2\xi}{5} - \frac{58M^2}{105} + \frac{\xi^2\beta_\lambda}{2} - \xi^2 \pm R_c + \frac{14M^2\xi^2}{3} - \frac{8M^2\xi^3}{3} + \frac{2M^2\xi^4}{3} - \frac{5\beta_\lambda \xi}{2} + \frac{2}{3}}{-\frac{2M^2\xi^6}{3} + 4M^2\xi^5 - \frac{49M^2\xi^4}{5} + \frac{188M^2\xi^3}{15} - \frac{62M^2\xi^2}{7} + \frac{116M^2\xi}{7} - \frac{65M^2}{126} + \xi^4\beta_\lambda - 4\xi^3\beta_\lambda + \frac{20\xi^2\beta_\lambda}{3} - \frac{16\xi\beta_\lambda}{3} + \frac{17\beta_\lambda}{15}}$$

and

$$R_c = \frac{1}{2}\left\{\begin{array}{l} \beta_\lambda^2\xi^4 - 4\beta_\lambda^2\xi^3 + 5\beta_\lambda^2\xi^2 - 2\beta_\lambda^2\xi + \frac{\beta_\lambda^2}{4} + \frac{152M^2\xi^4\beta_\lambda}{45} - \frac{608\xi^3M^2\beta_\lambda}{45} + \\ \frac{1924M^2\xi^2\beta_\lambda}{105} - \frac{3032M^2\beta_\lambda\xi}{315} + \frac{848M^2\beta_\lambda}{525} - 4\beta_\lambda\xi^4 + 16\xi^3\beta_\lambda - \frac{62\xi^2\beta_\lambda}{3} + \\ \frac{28\xi\beta_\lambda}{3} - \frac{4\beta_\lambda}{3} - \frac{52M^4\xi^4}{1575} + \frac{208M^4\xi^3}{1575} - \frac{172M^4\xi^2}{945} + \frac{472M^4\xi}{4725} - \frac{194M^4}{11025} + \frac{16M^2\xi^6}{3} - \\ 32M^2\xi^5 + \frac{3472M^2\xi^4}{45} - \frac{4288M^2\xi^3}{45} + \frac{19984M^2\xi^2}{315} - \frac{2272M^2\xi}{105} + \frac{928M^2}{315} + 4\xi^4 - 16\xi^3 \\ + \frac{64\xi^2}{3} - \frac{32\xi}{3} + \frac{16}{9} \end{array}\right\}^{0.5}.$$

In the same way, we derived the solution for the rough surface with variable thermal properties; however, they are too huge to be included in the paper.

FIN EFFICIENCY

The enhanced thermal performance of the micro-fin with the artificial surface could be established through the determination of the fin efficiency as this is considered as the key performance indicator in the analysis of fin thermal performance. In addition, following the definitions from our previous publications [25, 26], it could be deduced that the efficiency of the fin is given as

$$\eta = \frac{Q_f}{Q_{\max}} = \frac{\int_0^L \left[Ph(T)(T-T_a)\right]dx}{Ph(T)L(T_b - T_a)}. \quad (31)$$

Applying the dimensionless parameters, it can be shown that the dimensionless form of the efficiency is given as

$$\eta = \frac{Q_f}{Q_{\max}} = \int_0^L \theta_c^{n+1}(X)\,dX. \quad (32)$$

Ratio of the efficiency of the rough fin to the smooth fin can be stated as

$$\frac{\eta_{rf}}{\eta_{sf}} = \frac{\int_0^L \theta_{rf}^{n+1}(X)\,dX}{\int_0^L \theta_{sf}^{n+1}(X)\,dX}. \quad (33)$$

RESULTS AND DISCUSSION

Figures 4–9 depict the results of the Galerkin method of weighted residual. In Figure 4(a, b), the effects of geometrical ratio and nonlinear thermal conductivity term on the temperature distribution and, consequently, the heat dissipation capacity of the rough micro-fin. Although, it is shown in the figures that increase in the nonlinear thermal conductivity term causes an increase in the temperature distribution, it could be inferred as indicated that, as the geometrical ratio increases, the temperature of the micro-fin drops further which depicts enhanced thermal performance in the fin.

Effects of thermal conductivity of the rough micro-fins on the temperature distribution are displayed in Figure 5(a, b), when the thermo-geometric parameter is 0.5 and 1.0, respectively. It is indicated in the figure that the increase in the nonlinear thermal conductivity parameter reduces the rate of heat transfer in the micro-fin as the temperature of the fin drops when the value of the nonlinear thermal conductivity parameter increases. This same trend is recorded for the study of the effects of the thermo-geometric parameter on the thermal performance of the fin as shown in Figures 6 and 7. It should be noted that this result also represents the effects of increased thermal conductivity as depicted using different materials for improving the performance of the fin.

Also, it is shown in Figures 6 and 7 that the thermal efficiency of the micro-fin is significantly affected by the geometric ratio, nonlinear thermal conductivity parameter and the surface roughness of the micro-fin. It is indicated that geometric ratio and the surface roughness of the fin enhance its thermal performance. In addition, it could be said that the artificial rough surface creates a thin or thick layer on the fin (depending on the thickness of the roughness) and the base of the rough fin. This layer increases the thermal resistance of the solid–fluid interface with the heat flow thereby resulting in a higher temperature at the surface of the fin.

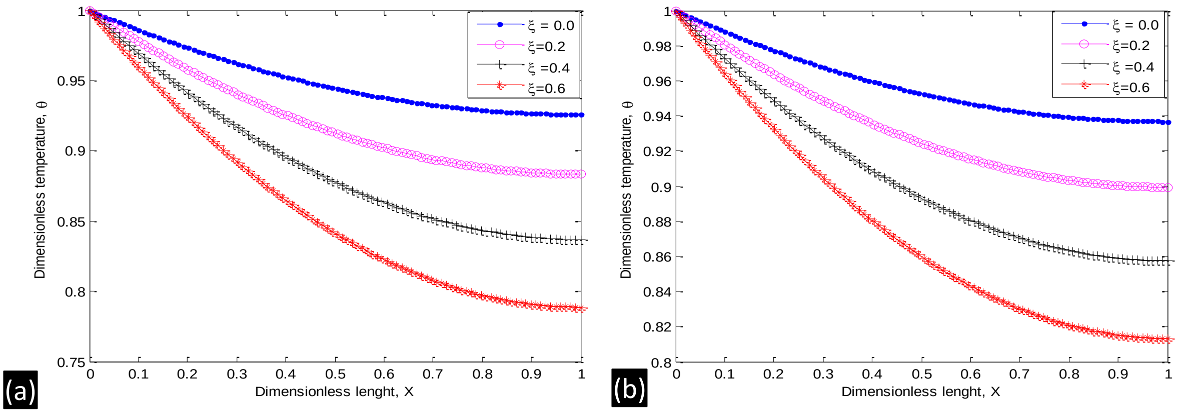

Fig. 4. *Effects of fouling Biot number on fin temperature when (a) β = 0.3 and (b) β = 1.0.*

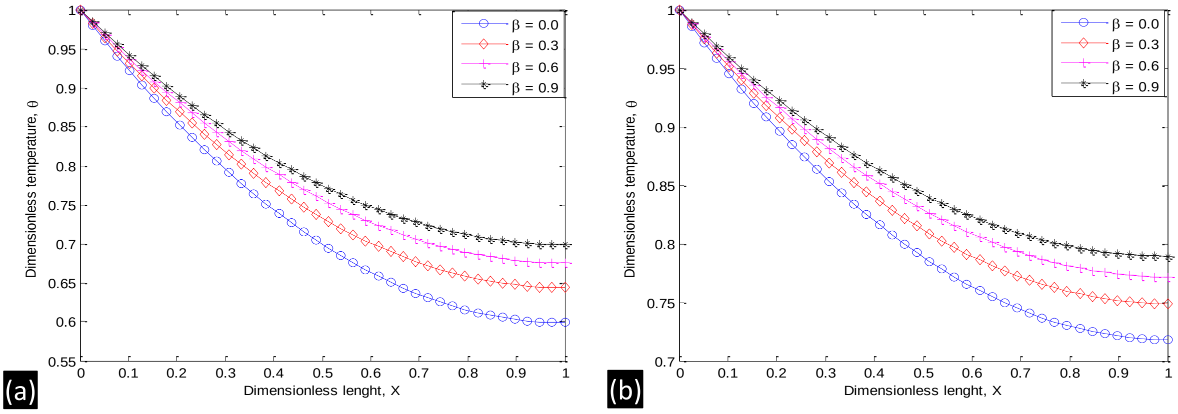

Fig. 5. *Effects of β on fin temperature when (a) M_c = 0.5 and (b) M_c = 1.0.*

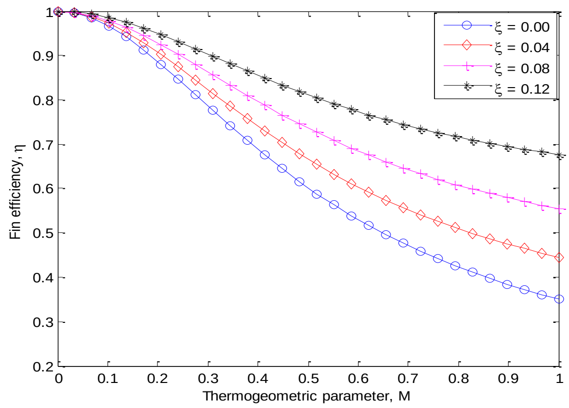

Fig. 6. *Effects of geometrical ratio on fin efficiency.*

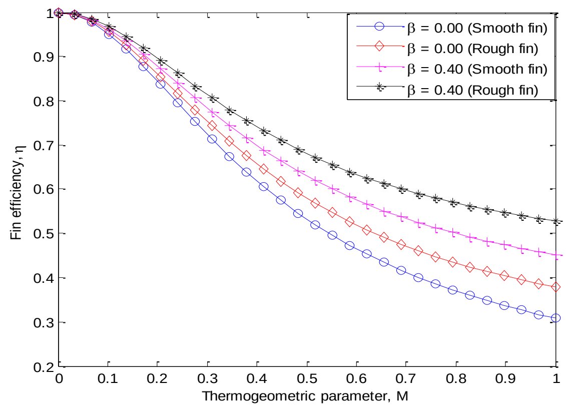

Fig. 7. *Effects of thermal conductivity and surface roughness on the efficiency of the micro-fin.*

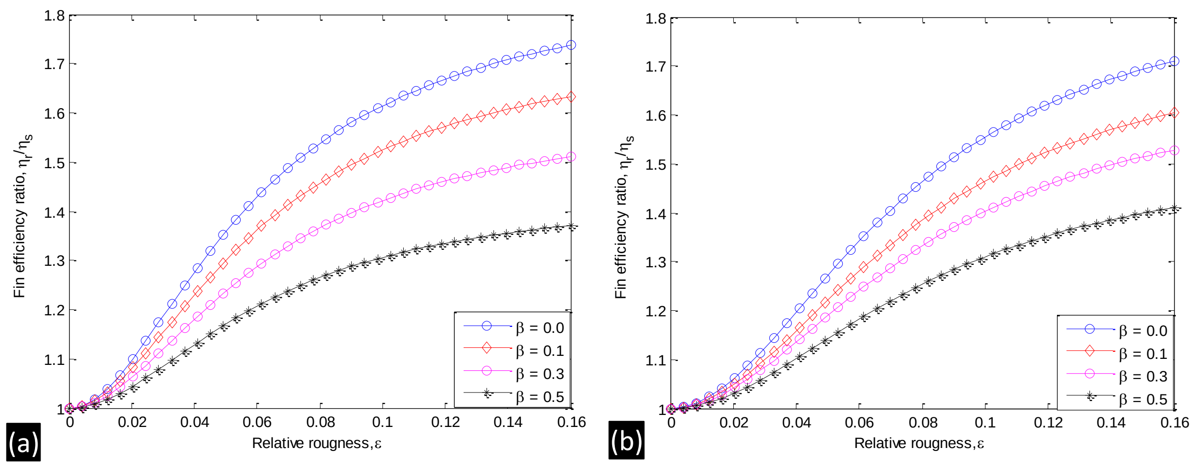

Fig. 8. *Effects of thermal conductivity on fin efficiency ratio when (a) M = 0.5 and M = 1.0.*

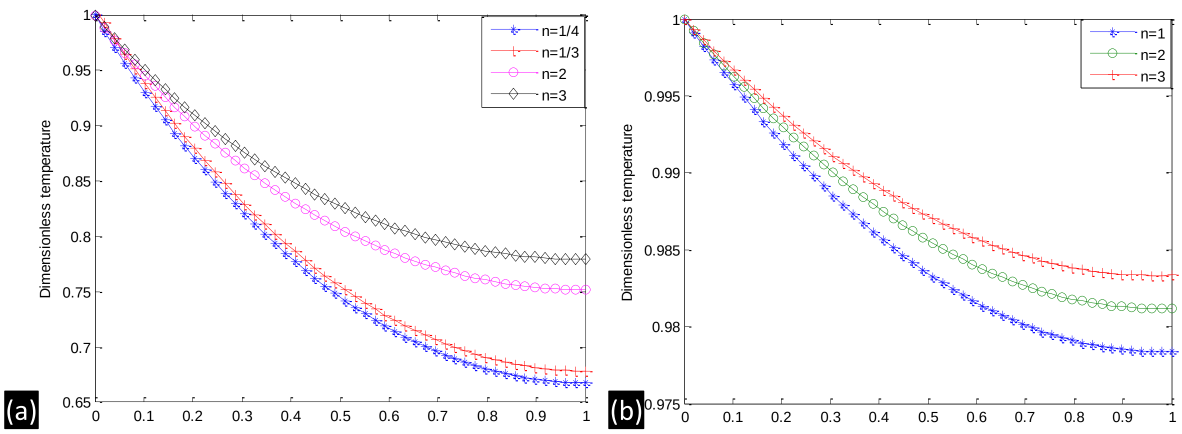

Fig. 9. *Dimensionless temperature distribution in the fin when (a) M = 1 and (b) M = 3.*

Figure 8(a,b) shows the effects of thermal conductivity and artificial surface roughness on the fin efficiency ratio. The fin efficiency ratio, which is the ratio of the efficiency of the rough fin to the efficiency of the smooth fin, is shown in the figure to be greater than unity. This depicts an enhanced thermal performance in the rough fin as compared to the smooth fin. The surface rough roughness of the fin increases the thermal efficiency of the fin due to the increase in temperature uniformity in the rough fin and increase in the temperature difference between the rough micro-fin and the bulk temperature.

Effects of multi-boiling constant on the temperature of the fin are shown in Figure 9(a, b). For the different values of the multi-boiling constant, it is depicted that the temperature distribution falls monotonically along the length of the extended surface. Also, the figure shows that more heat is transferred to the environment through the fin at the lower values of the multi-boiling parameter than at its higher values.

CONCLUSION

In this work, a study on enhanced heat transfer and thermal management of cylindrical micro-fins with artificial surface roughness has been presented using Galerkin method of weighted residual. The analytical solutions of the developed thermal models have been used to carry out parametric studies and to establish the thermal performance enhancement of the rough fins over the existing smooth fins. The results showed that geometric ratio and the surface roughness of the fin enhance its thermal performance. The fin efficiency ratio is always greater than unity when the rough and the smooth fins are subjected to the same operations with the same geometrical, physical, thermal and material properties. Therefore, we establish that improved thermal management of electronic and thermal systems could be achieved using artificial rough surface fins or heat sink.

NOMENCLATURE

A_b	Cross-sectional area at the fin base, m^2
A_c	Cross-sectional area of the fin, m^2
$\bar{A}_c$	Average cross-sectional area of the rough fin, m^2
A_s	Surface area of the fin exposed to convection, m^2
$\bar{A}_s$	Average surface area of the rough fin exposed to convection, m^2
B_i	Biot number, given by $2r_b h/k$
L	Fin length, m^2
m	Thermo-geometric parameter, m^{-1}
m_σ	Mean absolute surface slope
M^2	Extended Biot number,
n	Heat transfer coefficient constant
P	Fin perimeter, m
q	Heat transfer rate, W
r_δ	Random variation of the fin radius in the angular direction, m
r_b	Radius at the fin base, m
r_L	Random variation of the fin radius in the longitudinal direction, m
T	Temperature, K
T_b	Base temperature, K

GREEK SYMBOLS

$\mathcal{E}$	Relative roughness
η	Fin efficiency
λ	Length of the arc of the fin profile, m
θ	Dimensionless temperature
σ	Isotropic surface roughness, m
σ_δ	Fin surface roughness in the angular direction, m
σ_L	Fin surface roughness in the longitudinal direction, m
ξ	Geometric ratio
ψ	Dimensionless coordinate

REFERENCES

[1] Garimella SV, Fleischer AS, Murthy JY, Keshavarzi A, Prasher R, Patel C, Bhavnani SH, Venkatasubramanian R, Mahajan R, Joshi Y, Sammakia B, Myers BA, Chorosinski L, Baelmans M, Sathyamurthy P, Raad PE. Thermal challenges in next-generation electronic systems. *IEEE Trans Compon Packag Technol*. 2008; 31: 801–815p.

[2] Ventola L, Robotti F, Dialameh M, Calignano F, Manfredi D, Chiavazzo E, Asinari P. Rough surfaces with enhanced heat transfer for electronics cooling by direct metal laser sintering. *Int J Heat Mass Transf*. 2014; 75: 58–74p.

[3] Ligrani PM, Oliveira MM, Blaskovich T. Comparison of heat transfer augmentation techniques. *AIAA J*. 2003; 41: 337–362p.

[4] Xiang Rui Meng XLM, Lu JF, Wei XL. A study on improving in natural convection heat transfer for heat sink of high power LEDs. In: Fan W, editor. *Advanced Materials Research*: *Manufacturing Sceince and Technology*, *ICMST2011*. 2011, pp. 6834–6839.

[5] Shih CJ, Liu GC. Optimal design methodology of plate-fin heat sinks for electronic cooling using entropy generation strategy. *IEEE Trans Compon Packag Technol*. 2004; 27: 551–559p.

[6] Khan WA, Culham JR, Yovanovich MM. The role of fin geometry in heat sink performance. *J Electron Packag*. 2006; 128: 324–330p.

[7] Yang Y-T, Peng H-S. Numerical study of pin-fin heat sink with un-uniform fin height design. *Int J Heat Mass Transf*. 2008; 51: 4788–4796p.

[8] Wong W, Owen I, Sutcliffe CJ, Puri A. Convective heat transfer and pressure losses across novel heat sinks fabricated by Selective Laser Melting. *Int J Heat Mass Transf*. 2009; 52: 281–288p.

[9] Achenbach E. The effect of surface roughness on the heat transfer from a circular cylinder to the cross flow of air. *Int J Heat Mass Transf*. 1977; 20: 359–369p.

[10] Honda H, Takamastu H, Wei JJ. Enhanced boiling of FC-72 on silicon chips with micro-pin-fins and submicron-scale roughness. *J Heat Transf.* 2001; 124: 383–390p.
[11] Kalinin EK, Dreitser GA. Heat transfer enhancement in heat exchangers. In: Hartnett JP, Irvine TF, Cho YI, Greene GA, editors. *Advances in Heat Transfer*. Elsevier; 1998, Vol. 31, pp. 159–332.
[12] Zhou F, Catton I. Numerical evaluation of flow and heat transfer in plate-pin fin heat sinks with various pin cross-sections. *Numer Heat Transf Part A.* 2011; 60: 107–128p.
[13] Elyyan MA, Rozati A, Tafti DK. Investigation of dimpled fins for heat transfer enhancement in compact heat exchangers. *Int J Heat Mass Transf.* 2008; 51: 2950–2966p.
[14] Culham JR, Muzychka YS. Optimization of plate fin heat sinks using entropy generation minimization. *IEEE Trans Compon Packag Technol.* 2001; 24: 159–165p.
[15] Marques C, Kelly KW. Fabrication and performance of a pin fin micro heat exchanger. *J Heat Transf.* 2004; 126: 434–444p.
[16] Ventola L, Scaltrito L, Ferrero S, Maccioni G, Chiavazzo E, Asinari P. Micro-structured rough surfaces by laser etching for heat transfer enhancement on flush mounted heat sinks. *J Phys Conf Series.* 2014; 525: 012017.
[17] Zhou F, Catton I. Obtaining closure for a plane fin heat sink with elliptic scale-roughened surfaces for Volume Averaging Theory (VAT) based modeling. *Int J Therm Sci.* 2013; 71: 264–273p.
[18] Congshun W, Youmin Y, Simon T, Tianhong C, North MT. Microfabrication of short pin fins on heat sink surfaces to augment heat transfer performance. In: *13th InterSociety Conference on Thermal and Thermomechanical Phenomena in Electronic Systems*. 2012, pp. 944–950.
[19] Reimund N, Bernhard M, Mathias G, Thomas T. Additive manufacturing boosts efficiency of heat transfer components." *Assem Autom.* 2011; 31: 344–347p.
[20] Simchi A. Direct laser sintering of metal powders: mechanism, kinetics and microstructural features. *Mater Sci Eng A.* 2006; 428: 148–158p.
[21] Manfredi D, Calignano F, Krishnan M, Canali R, Ambrosio E, Atzeni E. From powders to dense metal parts: characterization of a commercial AlSiMg alloy processed through direct metal laser sintering. *Materials.* 2013; 6: 856p.
[22] Calignano F, Manfredi D, Ambrosio EP, Iuliano L, Fino P. Influence of process parameters on surface roughness of aluminum parts produced by DMLS. *Int J Adv Manuf Technol.* 2013; 67: 2743–2751p.
[23] Bahrami M, Yovanovich MM, Culham RJ. Role of random roughness on thermal performance of microfins. *J Thermophys Heat Transf.* 2007; 21: 153–157p.
[24] Díez LI, Espatolero S, Cortés C, Campo A. Thermal analysis of rough micro-fins of variable cross-section by the power series method. *Int J Therm Sci.* 2010; 49: 23–35p.
[25] Sobamowo MG. Thermal analysis of longitudinal fin with temperature-dependent properties and internal heat generation using Galerkin's method of weighted residual. *Appl Therm Eng.* 2016; 99: 1316–1330p.
[26] Sobamowo MG, Kamiyo OM, Adeleye OA. Thermal performance analysis of a natural convection porous fin with temperature-dependent thermal conductivity and internal heat generation. *Therm Sci Eng Progr.* 2017; 1: 39–52p.